

Configuration-interaction effects on the L and M Auger spectra of Cu and Zn[†]

E. J. McGuire

Sandia Laboratories, Albuquerque, New Mexico 87115

(Received 17 August 1977)

Configuration interaction (CI) effects are examined for both initial and final states in the L - and M -shell Auger spectra of Cu and Zn. CI accounts for the anomalous energy splitting of 1D and 3P terms in the $L_{2,3}$ - $M_{2,3}M_{2,3}$ Auger transition. At the same time CI increases the $L_{2,3}$ - $M_1M_{4,5}$ 1D transition rate, so that the 1D intensity is comparable to the 3D intensity. CI effects on the 1D double-vacancy lifetimes, while in the right direction, are not sufficient to account for the observed difference in L_3 - $M_1M_{4,5}$ 1D and 3D linewidths. CI effects cannot account for the discrepancy between calculated and measured M_1 and $M_{2,3}$ linewidths. It is hypothesized that the discrepancy arises from the use of Herman-Skillman rather than Hartree-Fock wave functions in the calculation of low-energy super Coster-Kronig matrix elements. With matrix elements adjusted via this hypothesis the M_1 - VV and $M_{2,3}$ - VV Auger line shapes are calculated for Cu. Further the L_3 - $M_{2,3}M_{2,3}$ and L_3 - $M_{2,3}M_{4,5}$ line shapes, including final-state lifetime effects, are calculated. The latter calculations indicate that a discrepancy between calculated and measured $L_{2,3}$ - MM configuration intensities is an experimental artifact.

I. INTRODUCTION

The L - and M -shell Auger spectra of Cu have attracted considerable interest,¹⁻¹² as the spectra exhibit both major and minor anomalies. The major anomaly is that the metallic $CuL_{2,3}$ - $M_{4,5}M_{4,5}$ spectrum is atomiclike and shows no effects of the $3d$ electron density of states. It has been hypothesized^{7,10,12} that the anomaly arises from the large correlation energy of two $3d$ holes localized on the same ion, compared to the relatively small $3d$ bandwidth. This is a final-state hypothesis and does not account for the absence of initial state effects. That is, with an atomiclike final state dominating the Auger electron energy distribution, one expects the atomiclike spectrum to be modulated by the initial-state $3d$ electron distribution function. The minor anomalies are questions that clearly can be addressed within an atomic physics framework. Specifically; (i) the measured splitting of the 3P and 1D terms in the $(3p)^4$ configuration is roughly twice the calculated splitting; (ii) the measured ratio¹³ of $L_{2,3}$ - $M_{2,3}M_{2,3}$: $L_{2,3}$ - $M_{2,3}M_{4,5}$: $L_{2,3}$ - $M_{4,5}M_{4,5}$ intensities is 14:30:56 in Zn while an average of two calculations^{14,15} is 24:34:42; and, (iii) the calculated M_1 and $M_{2,3}$ linewidths are larger than the measured values. It will be shown that the first minor anomaly is a direct consequence of final-state configuration interaction (CI) between the 1D terms of $(3s)^2(3p)^4(3d)^{10}$ and $(3s)^1(3p)^6(3d)^9$. The second minor anomaly appears to result from the background subtraction used in the Zn data analysis. By comparing the Zn measurements with a computed synthesized spectra, it will be shown that there is no anomaly.

The final minor anomaly requires a bit more

discussion. Earlier,¹⁶ I had calculated the M_1 and $M_{2,3}$ linewidths using one-electron orbitals for Cu and Zn atoms with an M -shell hole. The calculated values were a factor of 2 to 3 larger than measured photoelectron linewidths. Yin *et al.*⁵ calculated the M_1 and $M_{2,3}$ linewidths using a neutral-atom central potential to generate one-electron orbitals. Their calculations were in excellent agreement with the measurements. However, the rates for the dominant super Coster-Kronig transitions, M_1 - $M_{2,3}M_{4,5}$ and $M_{2,3}$ - $M_{4,5}M_{4,5}$, are strongly dependent on the choice of continuum electron energy and Yin *et al.*⁵ used energies significantly smaller than those deduced from recent measurements.⁷ I have reproduced the calculated M_1 and $M_{2,3}$ linewidths of Yin *et al.*⁵ with a neutral atom central potential and their energies, but with a neutral-atom central potential and experimental energies I find significantly larger linewidths. This suggests that configuration interaction may play a role. However, an examination of the M_1 - $M_{2,3}M_{4,5}$ and $M_{2,3}$ - $M_{4,5}M_{4,5}$ intensities in L - S coupling indicates that final state CI is not an important effect. That is the dominant final state terms are those of high L value [e.g., 3F and 1G in $(3d)^8$] and these terms are not found with the correct parity in other $n=3$ double vacancy states.

The possibility that initial state CI effects could affect the calculated M_1 and $M_{2,3}$ lifetimes was examined. That is in Cu the $(3s)^1(3p)^6(3d)^{10}(4s)^1S$, 3S terms can interact with the $[(3s)^2(3p)^4(3d)^{10}LS(4s)(nL)]^1S$, 3S terms. The conclusion reached is that the CI mixing is small, and that even if it were large it would have only a slight effect on the M_1 lifetime.

I conclude, then, that the absence of significant

CI effects on the Cu M_1 and $M_{2,3}$ lifetimes, and the good agreement between experimental widths and the calculation by Yin *et al.*⁵ using a low Auger electron energy, indicate that the source of error in the calculations is the exchange approximation in the Herman-Skillman¹⁷ wave functions. Kennedy and Manson¹⁸ have shown that the use of Hartree-Fock rather than Herman-Skillman wave functions significantly improves the calculated photoionization cross-sections of the noble gases near threshold. In effect the Hartree-Fock calculations inhibit the penetration of the continuum orbital into the core, compared to the Herman-Skillman wave functions. The net effect is that a Hartree-Fock continuum orbital is similar to a Herman-Skillman continuum orbital at a lower energy, consistent with the agreement between the calculations of Yin *et al.*⁵ and experiment.

This study of the origin of the discrepancy in the Cu M_1 and $M_{2,3}$ linewidths is necessary if one wishes to quantitatively calculate the M_1 and $M_{2,3}$ Auger spectra. Further, while the final state CI calculations do resolve the discrepancy between measured and calculated term energies in the L_{23} -MM Auger spectra, they lead to an additional difficulty. The $(3s)^2(3p)^4(3d)^{10} {}^1D$ intensity is reduced and the $(3s)^1(3p)^5(3d)^9 {}^1D$ intensity is enhanced due to CI. However, this is not seen experimentally. This suggests that there is an interference effect in the decay of the double-vacancy 1D terms, since both terms preferentially decay to the $(3s)^2(3p)^5(3d)^8$ configuration. But the calculation of this effect involves the same matrix elements (at slightly different energies) as in the decay of single M_1 and $M_{2,3}$ vacancies.

In Sec. II final-state CI effects are examined

TABLE I. Configuration interaction matrix elements for even-parity double-vacancy terms with $n=3$.

Hole config. \ Hole config.		1S		
		$[s]^2$	$[p]^2$	$[d]^2$
$[s]^2$		$2I(3s) + F^0(3s, 3s)$	$-\frac{1}{\sqrt{3}}R_1(ss, pp)$	$+\frac{1}{\sqrt{5}}R_2(ss, dd)$
$[p]^2$			$2I(3p) + F^0(3p, 3p)$ $+\frac{12}{25}F^2(3p, 3p)$	$-\sqrt{15}[\frac{2}{15}R_1(pp, dd) + \frac{3}{35}R_3(pp, dd)]$
$[d]^2$				$2I(3d) + F^0(3d, 3d)$ $+\frac{2}{7}(F^2(3d, 3d) + F^4(3d, 3d))$
Hole config. \ Hole config.		3P		
		$[p]^2$		$[d]^2$
$[p]^2$		$2I(3p) + F^0(3p, 3p)$ $-\frac{3}{25}F^2(3p, 3p)$		$-3\sqrt{5}[\frac{1}{15}R_1(pp, dd) - \frac{1}{35}R_3(pp, dd)]$
$[d]^2$				$2I(3d) + F^0(3d, 3d)$ $+\frac{1}{7}F^2(3d, 3d) - \frac{4}{21}F^4(3d, 3d)$
Hole config. \ Hole config.		1D		
		$[p]^2$	$[d]^2$	$[s][d]$
$[p]^2$		$2I(3p) + F^0(3p, 3p)$ $+\frac{3}{25}F^2(3p, 3p)$	$-\frac{3}{5\sqrt{21}}[\frac{7}{3}R_1(pp, dd) + \frac{3}{7}R_3(pp, dd)]$	$\frac{2}{\sqrt{15}}R_1(pp, sd)$
$[d]^2$			$2I(3d) + F^0(3d, 3d)$ $-\frac{3}{49}F^2(3d, 3d) + \frac{4}{49}F^4(3d, 3d)$	$-\frac{2}{\sqrt{35}}R_2(sd, dd)$
$[s][d]$				$I(3s) + I(3d)$ $+F^0(3s, 3d) + \frac{1}{5}G^2(3s, 3d)$

and it is shown that CI accounts for the anomalous term splitting in Cu and Zn. In Sec. III, initial-state CI effects are examined. In Sec. IV, the Cu $M_1-(M_{4,5})^2$ and $M_{2,3}-(M_{4,5})^2$ Auger spectra are calculated. In Sec. V, the double-vacancy 1D term decay rates are calculated, and in Sec. VI, the Cu $L_{23}-(M_{2,3})^2$, $L_{23}-M_{2,3}M_{4,5}$, and $L_{23}-(M_{45})^2$ spectra are synthesized, including final-state lifetimes, and compared with the measurements of Aksela and Aksela¹³ on Zn.

II. FINAL-STATE CONFIGURATION INTERACTION

Final state configuration interaction effects on Auger spectra were first studied by Asaad.¹⁹ He examined the effect of CI on the 1S_0 terms of $(2s)^0(2p)^6$ and $(2s)^2(2p)^4$ in K - LL spectra. For L - MM and M - MM spectra the filled $3d$ shell increases the number of terms that can interact, i.e., 1S from $[3s]^2$, $[3p]^2$ and $[3d]^2$, 3P from $[3p]^2$ and $[3d]^2$, and 1D from $[3p]^2$, $[3s][3d]$, and $[3d]^2$, (the brackets indicate hole notation). In Table I, are listed the configuration interaction matrix elements. The terms $I(nl)$, $F^j(nl, n'l')$, $G^j(nl, n'l')$ are standard electrostatic integrals appearing in the diagonal matrix elements. The terms $R_i(ab, cd)$ are also electrostatic integrals with $R_i(ab, ab) = F^i(a, b)$ and $R_i(aa, bb) = G^i(a, b)$. Many of the electrostatic integrals are available in Mann's tables.²⁰ Some are not and these I calculated by approximating with a series of seven straight lines the quantity $(-rV(r))$ of Herman and Skillman¹⁷ for neutral Cu. In Table II my calculated values are listed and compared with Mann's values when possible. The matrix elements are in Rydbergs.

For the ionization energies $I(nl)$, the values measured by Antonides *et al.*⁷, are used and for the electrostatic integrals, the values in Table II. In Table III, are listed the calculated term energies with and without CI. The principal measurable effect of CI is to increase the 1D - 3P splitting in $[3p]^2$ from 4.0 to 7.1 eV. Antonides *et al.* measure a splitting of 6.4 ± 0.5 eV, in reasonable agreement with the calculation including CI. The interesting feature is that the large CI effect is between the 1D terms of $[3p]^2$ and $[3s][3d]$. As a consequence the 1D - 3D splitting in $[3s][3d]$ is reduced from 5 eV without CI, to 2 eV with CI. Antonides *et al.* do not report on the $L_{23}-M_1M_{4,5}$ spectra of Cu, but Mariot and Dufour²¹ measure a $[3s][3d]$ 1D - 3D splitting of ≈ 4 eV in Zn, when the value calculated without CI is 7 eV.

Expressions for the Auger transition rate with CI mixing coefficients are listed in Table IV. Explicit evaluation of the $L_{2,3}$ transition rates (in units of $10^{-4}/\text{atu}$) are listed in Table V, both with

TABLE II. Electrostatic interaction matrix elements in Rydbergs for even-parity double-vacancy configurations with $n=3$. The first entries are from Mann's tables (Ref. 20).

Matrix element	$R_0(3s3s, 3s3s)$	$R_0(3p3p, 3p3p)$	$R_0(3d3d, 3d3d)$	$R_0(3s3d, 3s3d)$	$R_1(3p3p, 3p3p)$	$R_2(3d3d, 3d3d)$	$R_1(3d3d, 3d3d)$
Mann (Ref. 20)	2.494	2.390	1.909	2.159	1.194	0.8565	0.5280
Present	2.510	2.374	1.965	2.200	1.185	0.8841	0.5475
Matrix element	$R_2(3s3d, 3d3s)$	$R_1(3s3s, 3p3p)$	$R_2(3s3s, 3d3d)$	$R_1(3p3p, 3d3d)$	$R_3(3p3p, 3d3d)$	$R_1(3p3p, 3s3d)$	$R_2(3s3d, 3d3d)$
Mann (Ref. 20)	0.9138	1.617	0.9138	1.215	0.7308	1.384	0.8762
Present	0.9294	1.613	0.9301	1.226	0.7410	1.384	0.8762

TABLE III. Energy levels (in eV) for even-parity double-vacancy terms with $n=3$ in Cu, with and without configuration interaction.

Configuration	[s] ²		[p] ²		[d] ²			[s][d]	
	¹ S	³ S	³ P	¹ D	¹ S	³ P	¹ D	¹ D	³ D
Without CI	278.9	192.6	182.9	186.9	37.6	32.5	32.1	158.5	153.5
With CI	280.9	191.5	183.1	190.2	36.6	32.3	31.8	155.5	153.5

and without CI, and with orbitals for both the neutral Cu atom, and the Cu atom with an L -shell hole. From Table V, it is clear that CI has a slight effect on the $L_{2,3}$ Auger spectrum. The $[3s]^2$ ¹S intensity is reduced, as was found by Asaad¹⁹ in the $K-L_1L_1$ transition. However because the $[3s]^2$ ¹S term can decay by super Coster-Kronig transitions it is unlikely that the $L_{2,3}-M_1M_1$ transition can be observed in solid Cu and Zn. The other significant effect of CI is an increase in the $[3s][3d]$ ¹D rate as a consequence of its mixing with the ¹D term of $[3p]^2$.

The CI calculations predict that the ¹D to ³D intensity ratio in the $L_3-M_1M_{4,5}$ transition should increase from 0.5 without CI to 2.0 with CI. However in Zn Mariot and Dufour²¹ observe a relatively narrow ³D peak with intensity larger than the relatively broad ¹D peak. Further, as shown in

Table V the ³P to ¹D intensity ratio is 1.3 with CI for the $L_3-(M_{2,3})^2$ transition. However the measurements of Antonides *et al.*⁷ indicate a ratio close to, but less than 1.0.

This discrepancy can be accounted for if CI leads to an interference effect in the decay of the ¹D terms. Decay of the $(3s)^2(3p)^4(3d)^{10}$ ¹D vacancy is principally to the $(3s)^2(3p)^5(3d)^8$ configuration, while the $(3s)^1(3p)^6(3d)^9$ ¹D term principally decays to $(3s)^2(3p)^5(3d)^8$. If one neglects the $(3s)^2(3p)^6(3d)^8$ ¹D term, and writes for the other two ¹D terms

$$\Psi_i(^1D) = C_{1i} \Psi([3p]^2 ^1D) + C_{2i} \Psi([3s][3d] ^1D), \quad (1)$$

$$i = 1, 2,$$

then the Auger transition rate summed over all terms of $(3s)^2(3p)^5(3d)^8$ is given by

$$\begin{aligned}
 W_i = & C_{1i}^2 \left(\frac{76}{45} R_1(1122)^2 + \frac{18 \times 29}{35 \times 49} R_3(1122)^2 - \frac{24}{35} R_1(1122)R_3(1122) + \frac{28}{15} R_1(1322)^2 + \frac{64}{245} R_3(1322)^2 \right. \\
 & \left. - \frac{16}{35} R_1(1322)R_3(1322) + \frac{100}{343} R_3(1522)^2 \right) \\
 & + C_{2i}^2 \left[\frac{8}{5} R_1(0112)^2 + \frac{72}{125} R_2(0121)^2 - \frac{24}{25} R_1(0112)R_2(0121) \right. \\
 & \left. + \frac{9}{5} R_1(0312)^2 + \frac{108}{125} R_2(0321)^2 - \frac{36}{25} R_1(0312)R_2(0321) \right] \\
 & + C_{1i}C_{2i} \left(\frac{8}{15\sqrt{15}} [R_1(0112) - \frac{8}{5} R_2(0121)] [R_1(1122) + \frac{9}{14} R_3(1122)] + \frac{14}{25\sqrt{21}} [R_1(0312) - \frac{6}{5} R_2(0321)] \right. \\
 & \left. \times [13R_1(1322) + 3R_3(1322)] - \frac{42}{5\sqrt{21}} R_1(0312)[R_1(1322) - \frac{3}{7} R_3(1322)] \right). \quad (2)
 \end{aligned}$$

This expression was obtained from Eqs. (7) and (8) of Ref. (22).

However before evaluating Eq. (2) it is necessary to discuss both the choice of Auger electron energy and the matrix element calculation.

One final observation from Table V is that CI does not significantly affect the ratio of $L_{2,3}-M_{2,3}M_{2,3}$ to $L_{2,3}-M_{4,5}M_{4,5}$ decay rates and cannot

account for the observations of Aksela and Aksela¹³ on Zn.

III. INITIAL STATE CI EFFECTS ON M_1 AND $M_{2,3}$ HOLES

To do quantitative calculations in electron spectroscopy for comparison with accurate measurements, requires at a minimum that the gross fea-

TABLE IV. The Auger transition rate including configuration interaction mixing coefficients for even parity $L_{23}-MM$ transitions.

Term	Transition rate
1S	$3\{C([s]^2, ^1S)R_1(1100) - C([p]^2, ^1S)[\frac{1}{3}R_0(1111) + \frac{2}{15}R_2(1111) + (C([d]^2, ^1S)/\sqrt{15})(\frac{2}{3}R_1(1122) + \frac{3}{7}R_3(1122))\}^2$
3P	$3\{C([p]^2, ^3P)[R_0(1111) - \frac{1}{5}R_2(1111)] - [C([d]^2, ^3P)/\sqrt{5}](R_1(1122) - \frac{3}{7}R_3(1122))\}^2$
1D	$\frac{5}{3}\{-C([p]^2, ^1D)(R_0(1111) + \frac{1}{25}R_2(1111)) + [7C([d]^2, ^1D)/5\sqrt{21}] [R_1(1122) + \frac{3}{19}R_3(1122)] - [C([s][d], ^1D)/\sqrt{15}][R_1(1102) + R_1(1120)]\}^2$ $+ \frac{35}{2}\{(\frac{6}{25}\sqrt{7})C([p]^2, ^1D)R_2(1311) - (\frac{2}{35}\sqrt{3})C([d]^2, ^1D) [R_1(1322) + \frac{12}{7}R_3(1322)] + (1/\sqrt{105})C([s][d], ^1D)[R_1(1302) + \frac{3}{7}R_3(1320)]\}^2$

tures of the calculation be correct. For decay of the M_1 and $M_{2,3}$ vacancies in Cu one must be able to accurately calculate the linewidths. Earlier,⁴ I¹⁶ had calculated these linewidths with a central potential for the atom with an M -shell hole. The calculated widths were two to three times larger than the measurement of Yin *et al.*⁵ Yin *et al.*⁵ recalculated the widths with neutral atom wavefunctions and found excellent agreement with the measurements. Unfortunately, the agreement was due to an incorrect choice of Auger electron energy. Antonides *et al.*⁷ measure the L_3-M_1 and $L_3-M_{2,3}$ energy difference in Cu as 809.7 and 856.0, respectively. Since the $L_3-M_{2,3}M_{4,5}$ and $L_3-M_{4,5}M_{4,5}$ Auger electron energies are measured to be 842 and 918 eV, respectively, the $M_1-M_{2,3}M_{4,5}$ Auger electron energy is 32 eV, while the $M_{2,3}-M_{4,5}M_{4,5}$ Auger electron energy is 62 eV. Yin *et al.*⁵ used 18 and 44 eV, respectively.

TABLE V. Explicit evaluation of even parity $L_{2,3}-MM$ Auger transition rates in Cu, using both a neutral atom central potential and the potential for a Cu atom with a $2p$ vacancy (1 at.u. = 2.42×10^{-17} sec.).

Hole configuration	Term	Auger transition rate (10^{-4} /atu)			
		Without CI		With CI	
		Neutral	Ion	Neutral	Ion
[s] ²	1S	0.84	0.92	0.26	0.27
	3P	6.20	7.07	7.08	8.18
[p] ²	1S	24.8	29.2	25.2	29.5
	3P	21.4	24.9	19.4	22.3
[d] ²	1S	0.95	1.81	0.65	1.35
	3P	1.13	2.15	0.77	1.61
	1D	6.52	11.7	6.49	11.6
	3F	14.2	25.2	14.2	25.2
	1G	38.2	67.3	38.2	67.3
[s][d]	1D	0.72	0.99	2.93	3.69
	3D	1.37	2.10	1.37	2.10

Since it is well established that super Coster-Kronig transition rates depend strongly on the choice of Auger electron energy I have calculated the Auger transition rates at the measured Auger electron energy with both a neutral and ion potential, and with the neutral-atom potential at the energies used by Yin *et al.*⁵ The results are shown in Table VI.

The calculated M_1 width with the neutral-atom potential at 18 eV is in excellent agreement with both the measurement and calculation of Yin *et al.*⁵ My calculated $M_{2,3}$ width at 44 eV is higher than the calculation and measurement of Yin *et al.* However in both cases the trends are clear. With the neutral-atom potential the calculated widths increase with Auger electron energy at low energy, and one can find energy sufficiently low to attain agreement between calculation and measurement. A second point clearly emerging from Table VI is that the calculated widths are dominated by the 3F and 1F terms of $[3p][3d]$ and the 1G and 3F terms of $[3d]^2$. These terms do not involve final-state CI with terms arising from the configurations $[3s][3p]$, or $[3s]^2$, $[3s][3d]$ and $[3p]^2$.

To determine if initial-state configuration interaction effects could account for the inability of the calculation at the measured Auger electron energy to reproduce the measured linewidths, CI matrix elements were calculated for the configuration $(3s)^1(3p)^6(3d)^{10}(4s)$ interacting with $(3s)^2(3p)^4(3d)^{10}(4s)(nl)$, where $nl = 4s, 4d,$ and $5s$. The relevant matrix elements $R_1(3p3p, 3sni)$ were calculated to be 0.0936, 0.0616, and 0.0372 Ry, for $nl = 4s, 4d,$ and $5s$, respectively. Comparison with the matrix elements in Table II indicate that these are quite small, and unless there were an accidental degeneracy in energy, there would not be substantial mixing via CI.

Finally Table VI indicates that the terms that

TABLE VI. M_1 and $M_{2,3}$ Auger transition rates in Cu using both a central potential for a Cu atom with a 3s hole and a neutral atom potential. The rates are evaluated at both the experimental Auger electron energy and at energies used in Ref. (5).

M_1 -Transition rates				$M_{2,3}$ -Transition rates					
Configuration	Term	Ion (30 eV)	Neutral (30 eV)	Neutral (18 eV)	Configuration	Term	Ion (62 eV)	Neutral (62 eV)	Neutral (44 eV)
[3p][3d]	3F	880	484	216	[3d] ²	1G	1185	907	564
	1F	1145	492	185		3F	519	408	266
	3P	5.0	1.6	0.2		1D	161	120	113
	1P	98.0	119	135		3P	7.1	5.2	5.7
Total		2128	1097	536	1S	7.5	6.2	8.5	
[3d] ²	1G	133.0	109		[3d][4s]		38.2	24.2	24.2
	1D	12.0	13.9		Total		1918	1471	981
	1S	0.8	0.5		Γ (eV)		5.22	4.00	2.67
Total		146	123	123					
[3d][4s]		46	25.1	25.1					
[3p][4s]		113	85.9	85.9					
Total		2433	1331	770					
Γ (eV)		6.59	3.61	2.09					

dominate M_1 decay are the 3F and 1F terms of [3p][3d]. If there were substantial CI between the Cu $(3s)^1(3p)^6(3d)^{10}(4s)^1$ 1S term and the $(3s)^2(3p)^4(3d)^{10}(4s)^2$ 1S term [with the largest $R_1(4p4p, 3snl)$ value], then the first term will primarily decay to $(3s)^2(3p)^5(3d)^9 P'Q'(4s)PQ$, with $PQ = ^2F$. With C_1 the coefficient of the first 1S term and C_2 the coefficient of the second 1S term the Auger transition rate is given by $\frac{1}{2} |8.85 C_1 + 0.206 C_2|^2$ for $P'Q' = ^1F$, and by $\frac{3}{2} |5.08 C_1 + 0.625 C_2|^2$ for $P'Q' = ^3F$. The numerical factors are obtained from calculated Auger matrix elements at 30 eV. Even if there were substantial CI with $C_1 = C_2 = 0.707$, the transition rates would not be significantly modified from those given in Table VI.

The obvious conclusion is that initial-state CI does not significantly influence the calculated M_1 and $M_{2,3}$ linewidths. Ohno and Wendin²³ have recently done many body Hartree-Fock calculations on the $M_{2,3}$ linewidth in Br ($Z=35$) and Kr ($Z=36$), and find excellent agreement with the measurements of Svensson *et al.*²⁴ Ohno and Wendin suggest that my earlier calculations¹⁶ on Kr overestimated the $M_{2,3}$ width because double-vacancy final-state correlation energy was not included. While this is true it appears unlikely that, by itself, it accounts for the overestimate: For Cu, using the experimental Auger electron energy, my calculation overestimates the width. This suggests that the calculations of Ohno and Wendin²³ are in excellent agreement with the measurements because they not only include the correlation energy but also because they use Hartree-Fock matrix elements. As mentioned in the introduction, Kennedy and Manson¹⁸ found significant improvement in the near threshold photoionization cross-

section of the noble gases in going from Herman-Skillman¹⁷ to Hartree-Fock wave functions.

I conclude that calculations of Coster-Kronig and super Coster-Kronig transition rates with Herman-Skillman wave functions will lead to overestimates when the Auger electron energy is low. However for calculating the Cu $M_{2,3}-(M_{4,5})^2$ Auger spectra it is reasonable to use the matrix elements with low Auger electron angular momentum calculated at the experimental Auger electron energy, while for high angular momentum to use matrix elements calculated at a lower energy, but such as to bring the calculated and measured linewidths into agreement. This is done in the next section.

IV. $M_1-(M_{4,5})^2$ AND $M_{2,3}-(M_{4,5})^2$ AUGER SPECTRA OF Cu

In Table VII are listed matrix elements for the [3s]-[3p][3d] and [3p]-[3d]² super Coster-Kronig transitions in Cu at a variety of Auger electron energies. For both transitions the matrix elements involving an $l=1$ continuum electron do not significantly change with energy, while for $l=3$ and 5 the matrix elements do change significantly. Using the [p]-[d]² matrix elements at $\epsilon=40$ eV leads to an $M_{2,3}$ line width of 2.25 eV, in reasonable agreement with the measured values.⁵ In Fig. 1 the calculated $M_{2,3}-(M_{4,5})^2$ Auger spectra are shown using matrix elements (and widths) calculated at 40 and 60 eV. The term splittings of [3d]² are those of Ref. 11, the M_2-M_3 spin-orbit splitting used was 2 eV,⁷ and the instrumental resolution assumed was 0.25 eV.

Using the matrix elements at 40 eV (2.25-eV width) the calculations indicate a double peaked

TABLE VII. The variation with Auger electron energy of the matrix elements for $M_1-M_{2,3}M_{4,5}$ and $M_{2,3}-M_{4,5}M_{4,5}$ Auger transitions in Cu. The matrix elements use continuum orbitals normalized per Ry. The starred entries were obtained with the ion potential.

(eV)	[3s]-[3p][3d]				[3p]-[3d] ²				
	$R_1(0112)$	$R_2(0121)$	$R_1(0312)$	$R_2(0321)$	$R_1(1122)$	$R_3(1122)$	$R_1(1322)$	$R_3(1322)$	$R_3(1522)$
18	2.90	4.64	-4.41	-1.69	1.69	2.32	-4.29	-1.66	-0.077
30	2.85	4.15	-6.96	-3.14	1.73	2.07	-6.69	-2.91	-0.166
40	2.69	3.72	-8.93	-4.43	1.65	1.85	-8.51	-3.95	-0.267
44	2.66	3.58	-9.62	-4.92	1.63	1.78	-9.13	-4.33	-0.314
60	2.64	3.20	-12.12	-6.93	1.44	1.42	-11.57	-5.98	-0.570
75	2.164	2.568	-13.40	-8.193	1.34	1.26	-12.43	-6.65	-0.718
30*	2.73	3.50	-10.15	-5.52					
60*					1.62	1.52	-13.2	-7.10	-0.598

structure. The low-energy peak is $M_3-(M_{4,5})^2 {}^1G$ while the higher-energy peak is a superposition of $M_2-(M_{4,5})^2 {}^1G$ and $M_3-(M_{4,5})^2 {}^3F$ peaks with approximately equal intensity and separated by 1 eV. Using the matrix elements at 60 eV (4.00-eV width) the calculations (dashed curves in Fig. 1) show that the double peaked structure is washed out.

The $M_1-(M_{4,5})^2$ Auger spectra is dominated by transitions to the 1G final state term. In Fig. 2, the calculated Auger spectrum is shown for $\Gamma(M_1) = 2.09$ and 3.61 eV. In Fig. 1 the curves are normalized to contain equal area, but in Fig. 2 they are not as the increase in $\Gamma(M_1)$ is due to the

$M_1-M_{2,3}M_{4,5}$ transition, not the $M_1-(M_{4,5})^2$ transition.

V. WIDTH OF THE DOUBLE VACANCY 1D TERMS

The calculation of the decay rate of the double-vacancy 1D terms introduces three difficulties; the Auger energy, which has not been measured; the choice of matrix elements; and the appropriate formalism. To calculate the decay rate of the double-vacancy 1D terms of $[3s][3d]$ and $[3p]^2$, it is necessary to estimate the Auger electron energy of the $[3s][3d] \rightarrow [3p][3d]^2$ and $[3p]^2 \rightarrow [3p][3d]^2$ transitions which are the dominant ones. We

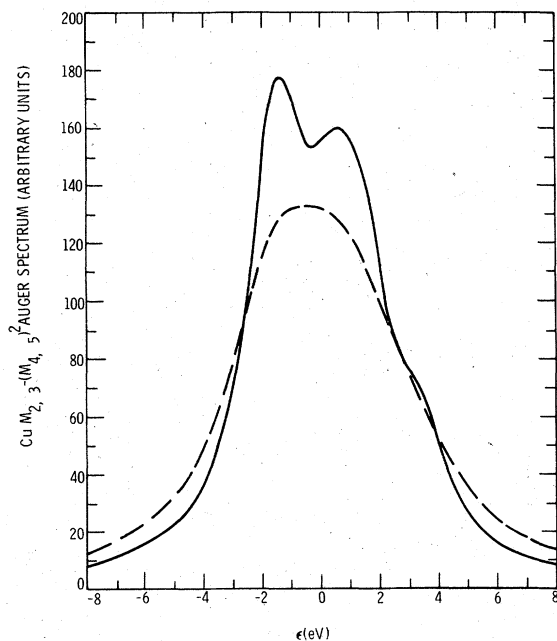


FIG. 1. The $M_{2,3}VV$ Auger spectrum of Cu. The solid (dashed) curve is obtained with $M_{2,3}-M_{4,5}M_{4,5}$ matrix elements at 40 (62) eV, and the calculated linewidth is 2.25 (4.00) eV.

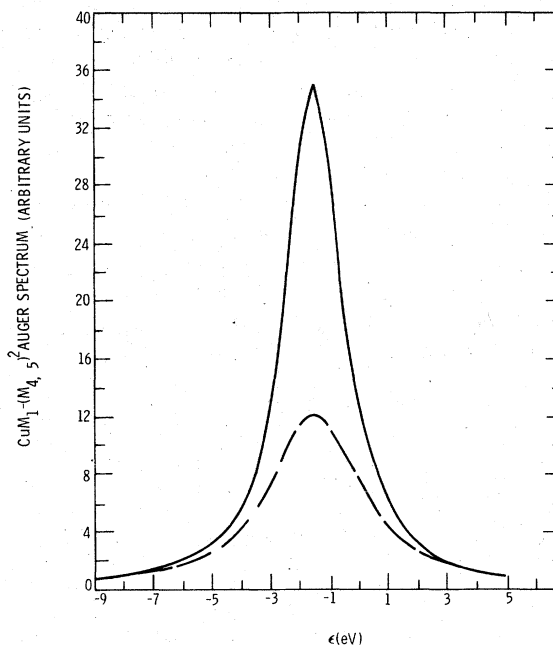


FIG. 2. The M_1-VV Auger spectrum of Cu. The solid (dashed) curve is obtained with $M_1-M_{2,3}M_{4,5}$ matrix elements at 18 (30) eV, and the calculated linewidth is 2.09 (3.61) eV.

estimate these energies via

$$E(M_1 M_{4,5} - M_{2,3} M_{4,5}^2) \\ \approx E(M_1 M_{4,5}) - E(M_{2,3} M_{4,5}) - [E(M_{4,5}^3) - E(M_{4,5}^2)]$$

and

$$E(M_{2,3}^2 - M_{2,3} M_{4,5}^2) \\ \approx E(M_{2,3}^2) - E(M_{2,3} M_{4,5}) - [E(M_{4,5}^3) - E(M_{4,5}^2)]$$

The first two entries on the right-hand side of the above expressions are obtained from Schön's measurements² of the L - MM Auger spectra. The additional term, the energy required to remove a $3d$ electron from a double ionized Cu ion was obtained from the L_1 ionization threshold (1096 eV), the assignment²⁵ of the measured Auger peak at 153 eV to the L_1 - $L_3 M_{4,5}$ transition, and the assignment of the $L_3 M_{4,5} - (M_{4,5})^3$ satellite spectra.¹¹ This leads to $E(M_{4,5}^3) - E(M_{4,5}^2) \approx 15$ eV, and to the estimate that the $M_1 M_{4,5} - M_{2,3} (M_{4,5})^2$ and $(M_{2,3})^2 - (M_{2,3})(M_{4,5})^2$ spectra are at approximately the energy of the $M_1 - M_{2,3} M_{4,5}$ and $M_{2,3} - M_{4,5}^2$ Auger transitions, i.e., 30 and 60 eV, respectively.

In double-vacancy decay, the ion is doubly charged in the initial state and triply charged in the final state. For single-vacancy decay, it was concluded in Sec. III that an accurate calculation of the M_1 and $M_{2,3}$ lifetime required Hartree-Fock rather than Herman-Skillman wave functions. Does double-vacancy super Coster-Kronig decay also require Hartree-Fock calculations? Since I cannot answer this question, I calculate the double-vacancy decay rates with neutral-atom matrix elements at both the estimated Auger energy and at the lower energies which led to good agreement with the measurements for M_1 and $M_{2,3}$ decay.

Finally the formalism used to calculate the double-vacancy decay rate is perturbation theory. That is, with the Hamiltonian given by $H = H_0 + V$, where V is the electrostatic interaction, and $|1\rangle$ and $|2\rangle$ are discrete eigenfunctions of H_0 and $|\epsilon\rangle$ is a continuum eigenfunction of H_0 , one has

$$\langle i | H_0 | j \rangle = E_i \delta_{ij} \quad \langle i | H_0 | \epsilon \rangle = 0,$$

$$\langle i | V | j \rangle = V_{ij}, \quad \langle i | V | \epsilon \rangle = V_{i\epsilon}.$$

If we use CI eigenfunctions,

$$|a\rangle = C_1 |1\rangle + C_2 |2\rangle, \quad |b\rangle = -C_2 |1\rangle + C_1 |2\rangle,$$

such that

$$\langle a | H_0 | b \rangle = E_a \delta_{a,b}, \quad \langle a | V | b \rangle = V_{aa} \delta_{a,b},$$

then

$$\langle a | V | \epsilon \rangle = C_1 V_{1\epsilon} + C_2 V_{2\epsilon}.$$

That is, the lifetime of a is determined by matrix

elements calculated at E_1 and E_2 , not matrix elements calculated at E_a . Since the transition rates are large, perturbation theory is suspect. A more accurate treatment begins with the levels $|a\rangle$ and $|b\rangle$ interacting with the continua.^{26,27} However, there are many interacting continua in $\{[(3p)^5 2P(3d)^8 P_4 Q_4] PQ + e\}^1 D$, which greatly complicates the analysis. Since Hartree-Fock matrix elements are not available, the more accurate calculations were not done.

The rate for the $[3s][3d]^3 D \rightarrow [3p][3d]^2$ transition summed over final states is given by Eq. (10) of Ref. 28. With the matrix elements evaluated at 18 eV, the contribution of the above transition to the $^3 D$ width is 1.34 eV. In the absence of CI the contribution of the $[3s][3d]^1 D \rightarrow [3p][3d]^2$ transition to the $^1 D$ lifetime is 1.24 eV. The difference in width is a multiplet effect. Yin *et al.*⁴ report a Cu L_3 photoelectron width of 0.54 eV. Then the calculation predicts a width of 1.88 eV for the $L_3 - M_1 M_{4,5}^3 D$ Auger peak.

With the Auger matrix elements at 18 and 30 eV, Eq. (2) becomes

$$\Gamma(^1 D) = 4.98 C_{1i}^2 + 1.24 C_{2i}^2 - 0.73 C_{1i} C_{2i}.$$

Inserting the calculated mixing coefficients $C_{11} = 0.9537$, $C_{12} = 0.2979$ for $[3p]^2 ^1 D$ and $C_{21} = 0.2988$, $C_{22} = 0.9541$ for $[3s][3d]^1 D$ we find the $[3s][3d]^1 D$ width increased from 1.24 to 1.78 eV, using the matrix elements at 18 and 30 eV. The $[3p]^2 ^1 D$ width is reduced from 4.98 to 4.43 eV. While the effect of CI on double-vacancy lifetimes are in the right direction to bring the calculations into agreement with the measurements, they are quantitatively too small.

Next, the calculations were done with the neutral-atom matrix elements at 30 and 60 eV. With the matrix elements at 30 eV and neglecting CI, the $[3s][3d]^3 D$, $^1 D$ widths are 2.76 and 2.48 eV, respectively. With CI the width is given by

$$\Gamma(^1 D) = 7.87 C_{1i}^2 + 2.48 C_{2i}^2 - 1.71 C_{1i} C_{2i}.$$

The $[3s][3d]^1 D$ width is increased from 2.48 to 3.45 eV, while the $[3p]^2 ^1 D$ width is reduced from 7.87 to 6.89 eV.

In summary, with CI and the lower-energy matrix elements the $^3 D$ and $^1 D$ terms of $L_3 - M_1 M_{4,5}$ have calculated linewidths of 1.88 and 2.32 eV, respectively, while with the higher-energy matrix elements they are 3.30 and 3.99 eV, respectively. Tentative measurements of Mariot and Dufour²⁹ are 2.0 and 3.2 eV, respectively.

The conclusion reached is while these calculations show that CI does affect the $^1 D$ double-vacancy lifetimes, they do not lead to quantitative agreement with the measurements. In particular, they do not account for the relatively small and

broad $[3s][3d] \ ^1D$ peak in the $L_3-M_1M_{4,5}$ Auger spectra of Cu and Zn. It is possible that more accurate calculations would lead to better agreement.

VI. $L_3-M_{2,3}M_{2,3}$ AND $L_3-M_{2,3}M_{4,5}$ AUGER SPECTRA OF Cu AND Zn

In their measurements of the L - MM Auger spectra of atomic Zn Aksela and Aksela¹³ find the $L_{23}-M_{23}M_{23}:L_{23}-M_{23}M_{45}:L_{23}-M_{4,5}M_{4,5}$ intensity ratios in Zn to be 14:30:56, while an average of two calculated^{14,15} values is 24:34:42. I suggest that the difference arises because of the background subtraction and the resulting error introduced in integrating the area under the peaks.

In the fourth column of Table VIII, are listed the calculated transition rates from an L_3 vacancy

TABLE VIII. Initial population of Cu double vacancy resulting from decay of an L_3 vacancy, relative energies within the double-vacancy configuration, and double-vacancy lifetimes using large and small matrix elements as described in the text.

Configuration	Term	E_{Rel} (eV)	I	Γ (eV)	
				Small	Large
$M_{2,3}M_{2,3}$	1S_0	-7.79	8.2	4.98	7.87
	3P_0	0.62	1.7	4.98	7.87
	3P_1	1.28	7.4	4.98	7.87
	3P_2	2.62	20.6	4.98	7.87
	1D_2	-5.15	22.3	4.43	6.89
$M_{23}M_{45}$	3F_4	5.11	0.26	1.10	1.74
	3F_3	4.22	0.12	1.10	1.74
	3F_2	3.55	0.04	1.10	1.74
	1F_3	-9.02	43.4	2.59	4.04
	3D_3	-1.09	13.1	2.82	4.47
	3D_2	-1.42	7.3	2.82	4.47
	3D_1	-1.64	3.6	2.82	4.47
	1D_2	3.59	1.1	1.96	3.13
	3P_2	-0.87	4.7	2.21	3.48
	3P_1	-0.21	3.0	2.21	3.48
	3P_0	0.13	1.0	2.21	3.48
	1P_1	-7.85	11.6	2.14	3.35
	$M_{4,5}M_{4,5}$	1G	-1.57	67.3	
3F		1.45	25.2		
1D		-0.47	11.6		
3P		-0.89	1.6		
1S		-6.00	1.2		

to various MM double vacancy final states. The matrix elements used were obtained with the ion potential,¹¹ and lead to configuration intensities of 23:35:42 (with the neutral-atom potential my calculations underestimate the $L_3-M_{2,3}M_{4,5}$ and $L_3-M_{4,5}M_{4,5}$ intensities compared to those of Ref. 14). The relative energies within a configuration are listed in column 3 of Table VIII. They were obtained using Mann's electrostatic integrals,²⁰ and the diagonal spin-orbit interaction matrix elements. Note that the $^1D_2-^3P_2$ splitting in $(M_{2,3})^2$, (the two strong terms), has been increased to 7.77 eV. The two lifetime estimates for the $(M_{2,3})^2$ terms are discussed in Sec. V. The lifetime estimates for the $M_{2,3}M_{4,5}$ terms are from Eq. (20) of Ref. 28, with the matrix elements at 44 and 60 eV. The synthesized $L_3-M_{2,3}M_{2,3}$ and $L_3-M_{2,3}M_{4,5}$ spectra are shown in Figs. (3) and (4).

From Figs. 1 and 2 of Ref. 13, I estimate the intensity of the measured Zn $L_3M_{4,5}M_{4,5} \ ^1G$, $L_3M_{2,3}M_{4,5} \ ^1F$, and $L_3M_{2,3}M_{2,3} \ ^1D$ peaks as 34, 15, and 6 respectively (where the units are $\frac{1}{20}$ inch). In a later analysis of their $L_3-M_{4,5}M_{4,5}$ spectrum, Aksela *et al.*³⁰ determine that their $L_3-M_{4,5}M_{4,5} \ ^1G$ line was 1.0-eV wide, with 0.5 eV from the

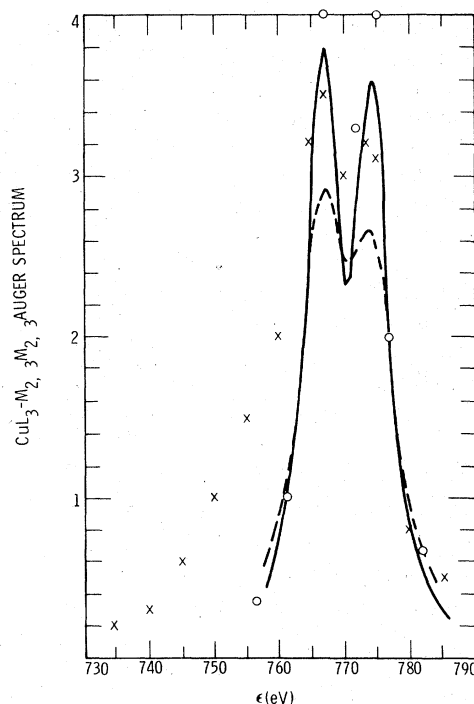


FIG. 3. The calculated $L_3-M_{2,3}M_{2,3}$ Auger spectrum of Cu. The solid (dashed) curve uses matrix elements at 40 (62) eV to compute the double-vacancy linewidth. The crosses are measured values from Ref. 7 and the open circles are Zn vapor measurements from Ref. 13, shifted in energy to overlap the Cu spectrum.

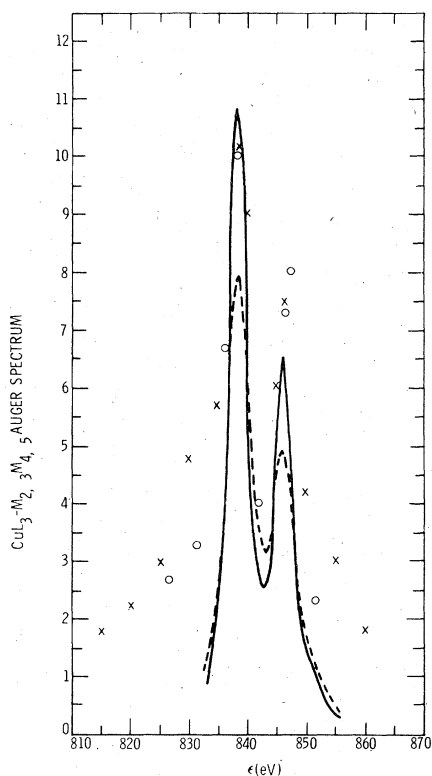


FIG. 4. The calculated $L_3-M_{2,3}M_{4,5}$ Auger spectrum of Cu. The solid (dashed) curve uses matrix elements at 18(30) eV to compute the double-vacancy linewidth. The crosses are measured values from Ref. 7 and the open circles are Zn vapor measurement from Ref. 13, shifted in energy to overlap the Cu spectrum.

spectral resolution and 0.5 ± 0.15 from the L_3 linewidth. Thus the area under their $L_3-M_{4,5}M_{4,5}^1G$ peak is 34, in the above units. This implies an Auger transition rate for $L_3-M_{4,5}M_{4,5}^1G$ of 68. The rate for this transition in Table 8 is 67.3. Thus one can directly compare the normalized intensities in Figs. 3 and 4 with the results of Aksela and Aksela¹³ with a $\frac{1}{20}$ -inch scale.

For the $L_3M_{2,3}M_{4,5}^1F$ and $L_3M_{2,3}M_{2,3}^1D$ peaks the synthesis leads to 11 and 4, while the measured values are 15 and 6. Thus even though the calculated configuration intensity ratios were used, and the minimum calculated linewidths, the calculated peaks are smaller than those observed. Then, if the $L_3-M_{2,3}M_{2,3}$ and $L_3-M_{2,3}M_{4,5}$ line shapes are consistent with the calculations, the measured $L_3-M_{2,3}M_{2,3}/L_3-M_{2,3}M_{4,5}$ and $L_3-M_{2,3}M_{4,5}/L_3-M_{4,5}M_{4,5}$ intensity ratios must be larger than that obtained by Aksela and Aksela.¹³ The low ratios then result from the background subtraction and/or the integration of the area under the peaks.

The solid curves in Figs. (3) and (4) were cal-

culated with the smaller linewidths, and the dashed curves with the larger linewidths. The principal difference in both calculations is the size of the minimum relative to the maximum. Also shown are the measurements of Antonides *et al.*⁷ on Cu (crosses), for which the energy scale is appropriate, and the measurements of Aksela and Aksela¹³ on Zn vapor (open circles), shifted in energy so the $L_3-M_{2,3}M_{2,3}^1D$ and $L_3-M_{2,3}M_{4,5}^1F$ peaks overlap the Cu peaks. While the measured minima and maxima intensity favor the larger linewidth calculation for $L_3-M_{2,3}M_{2,3}$, and the smaller linewidth calculation for $L_3-M_{2,3}M_{4,5}$, experimental and computational inaccuracies may be important.

In the region of the large peaks there is reasonable agreement in shape between the calculations and the measurements of Aksela and Aksela on Zn. My conclusion is that their measurements are consistent with the theoretical configuration intensity ratios.

The curious feature in Figs. 3 and 4 are the low-energy tails. These are seen by Antonides *et al.*⁷ for both solid Cu and solid Zn in both the $L_3-M_{2,3}M_{2,3}$ and $L_3-M_{2,3}M_{4,5}$ spectra. But for Zn vapor Aksela and Aksela do not see the tail in the $L_3-M_{2,3}M_{2,3}$ spectra. Since there will inevitably be satellite structure from L_1 Coster-Kronig decay, this suggests that Aksela and Aksela have overestimated the background correction on the low-energy side of the $L_3-M_{2,3}M_{2,3}$ spectra.

VII. CONCLUSIONS

The aim of these calculations was to predict the M_1-VV and $M_{2,3}-VV$ Auger spectra of Cu for comparison with measurements. But calculations of the M_1 and $M_{2,3}$ linewidths at the experimentally determined Auger electron energies considerably overestimated the linewidths. This suggested that CI effects might be responsible, but it was found that neither initial- nor final-state CI effects were significant in the M_1 and $M_{2,3}$ linewidth calculation. This, and results from photoionization cross-section calculations, strongly suggest the hypothesis is that the discrepancy in M_1 and $M_{2,3}$ linewidths arises from the use of Herman-Skillman rather than Hartree-Fock wave functions. If the hypothesis is proven valid it could account for some of the disagreement between calculated and measured M - and N -shell widths arising from super Coster-Kronig transitions. By eliminating the possibility that CI significantly affects the M_1 and $M_{2,3}$ linewidths in Cu and hypothesizing that Herman-Skillman matrix elements at an Auger energy somewhat lower than that measured were ap-

appropriate. the Cu M_1 - VV and $M_{2,3}$ - VV were calculated. They will be compared with experiment elsewhere.³¹

Final-state CI effects were shown to play a role in the Cu and Zn L - MM Auger spectra, with the largest effect being an increase in the 1D - 3P term splitting in the $M_{2,3}M_{2,3}$ double-vacancy configuration, and a decrease in the 1D - 3D term splitting in the $M_1M_{4,5}$ configuration. This is in agreement with measurements in Cu and Zn. Due to CI the $(M_{2,3})^2$ 1D intensity and linewidth are decreased relative to the $(M_{2,3})^2$ 3P peak. Calculations including spin-orbit splitting of the 3P_J terms are in agreement with the measurements. To compensate for this decrease the $M_1M_{4,5}$ 1D intensity and linewidth is increased relative to the $M_1M_{4,5}$ 3D peak. However the calculated $M_1M_{4,5}$ 1D intensity is increased too much and the linewidth too little, to agree with the measurements. This could be due to the use of an inappropriate formalism to calculate the $M_1M_{4,5}$ double vacancy linewidth.

The calculations here and in a later paper¹¹ emphasize the major anomaly in the Auger spectra

of metallic Cu, the complete absence of effects due to the $3d$ electron bandwidth. These calculations have explained some minor anomalies, but have pointed out two others. They are, first, the incompatibility of the Cu L_2 photoelectron linewidth measurement and the L_3 - $M_{4,5}M_{4,5}$ satellite spectral intensity, and, second, the intensity and width of the L_3 - $M_1M_{4,5}$ Auger peak.

Note added in proof. Weightman³² (Liverpool) has suggested that the peak identified as L_3 - $M_1M_{4,5}$ 1D is actually L_2 - $M_{2,3}M_{2,3}$ 3P , and the peak identified as L_3 - $M_1M_{4,5}$ 3D is actually L_3 - $M_1M_{4,5}$ 1D . If so, the anomaly concerning the L_3 - $M_1M_{4,5}$ linewidths vanishes, but, unfortunately, so has the L_3 - $M_1M_{4,5}$ 3D peak.

ACKNOWLEDGMENT

The progress of these calculations met with several unpleasant surprises and would not have been completed without the constant encouragement of H. Madden.

*This work was supported by the Energy Research and Development Administration.

¹L. I. Yin, T. Tsang, I. Adler, and E. Yellin, *J. Appl. Phys.* **43**, 3464 (1972).

²G. Schön, *J. Electron. Spectrosc.* **1**, 377 (1972).

³S. P. Kowalczyk, R. A. Pollak, F. R. McFeely, L. Ley, and D. A. Shirley, *Phys. Rev. B* **8**, 2387 (1973).

⁴L. I. Yin, I. Adler, M. H. Chen, and B. Crasemann, *Phys. Rev. A* **7**, 897 (1973).

⁵L. I. Yin, I. Adler, T. Tsang, M. H. Chen, D. A. Ringers, and B. Crasemann, *Phys. Rev. A* **9**, 1070 (1974).

⁶E. D. Roberts, P. Weightman, and C. E. Johnson, *J. Phys. C* **8**, L301 (1975).

⁷E. Antonides, E. C. Janse, and G. A. Sawatzky, *Phys. Rev. B* **15**, 1669 (1977).

⁸E. Antonides, E. C. Janse, and G. A. Sawatzky, *Phys. Rev. B* **15**, 4596 (1977).

⁹P. A. Feibelman and E. J. McGuire, *Phys. Rev. B* **15**, 3575 (1977).

¹⁰P. A. Feibelman, *Bull. APS* **22**, 432 (1977).

¹¹E. J. McGuire, *Phys. Rev. A* (to be published).

¹²L. I. Yin, T. Tsang, and I. Adler, *Phys. Rev. B* **15**, 2974 (1977).

¹³S. Aksela and H. Aksela, *Phys. Lett.* **48A**, 19 (1974).

¹⁴D. L. Walters and C. P. Balla, *Phys. Rev. A* **4**, 2164 (1971).

¹⁵E. J. McGuire, *L-Shell Auger, Coster-Kronig, and Radiative Matrix Elements*, Sandia Research Report,

SC-RR-71-0075.

¹⁶E. J. McGuire, *Phys. Rev. A* **5**, 1043 (1972).

¹⁷F. Herman and S. Skillman, *Atomic Structure Calculations* (Prentice-Hall, Englewood Cliffs, N.J., 1963).

¹⁸D. J. Kennedy and S. T. Manson, *Phys. Rev. A* **5**, 227 (1972).

¹⁹W. N. Asaad, *Nucl. Phys.* **66**, 494 (1965).

²⁰J. B. Mann, Los Alamos Scientific Laboratory Report, LASL-3690, 1967 (unpublished).

²¹J. M. Mariot and G. Dufour, *J. Phys. C* **10**, L213 (1977).

²²E. J. McGuire, *Phys. Rev. A* **12**, 330 (1975).

²³M. Ohno and G. Wendin, *Solid State Commun.* (to be published).

²⁴S. Svensson, N. Martensson, E. Basilier, P. A. Malmqvist, U. Gellius, and K. Siegbahn, *Physica Scripta* **14**, 141 (1976).

²⁵H. Madden (private communication).

²⁶U. Fano, *Phys. Rev.* **124**, 1866 (1961).

²⁷F. H. Mies, *Phys. Rev.* **175**, 164 (1968).

²⁸E. J. McGuire, *Phys. Rev. A* **10**, 32 (1974).

²⁹J. M. Mariot and G. Dufour (private communication).

³⁰S. Aksela, J. Väyrynen, and H. Aksela, *Phys. Rev. Lett.* **33**, 999 (1974).

³¹H. Madden, D. M. Zehner, and J. R. Noonan (to be published).

³²P. Weightman (private communication).